www.cadanda.com
Computer-Aided Design AND APPLICATIONS™

Evaluation of 3D Data Compression and Retrieval Method Based on Curve Mesh Filling

Gulibaha Silayi[1], Tsutomu Kinoshita[2], Yuta Muraki[3], Katsutsugu Matsuyama[4] and Kouichi Konno[5]

[1]Iwate University, gulbahar@lk.cis.iwate-u.ac.jp
[2]University of Niigata Prefecture, PXW05066@nifty.com
[3]Osaka Institute of Technology, muraki@is.oit.ac.jp
[4]Iwate University, matsuyama@eecs.iwate-u.ac.jp
[5]Iwate University, konno@eecs.iwate-u.ac.jp

ABSTRACT

Digital mock-up (DMU) and/or compound document with 3D data are one of the most important methods to represent a product model. Since the data size of 3D models becomes greater year by year, 3D data compression and retrieval algorithm is required to easily exchange such information through the Internet. Because broadband is still not popular in some regions in the world, it is necessary to send huge data in a small size as much as possible. Therefore, in this paper we developed an application system that transfers 3D surface models and then the performance of the 3D surface compression and retrieval algorithm is evaluated.

Keywords: 3D surface model, 3D data compression, curve mesh interpolation, N-side filling method, B-spline surface.

1. INTRODUCTION

Manufacturing has been globalized during the last two decades. Designed and manufactured by the manufacturing facilities around the world have been routinely performed. From a manufacturer's perspective, 3D data is beneficial information because it allows visualization of exactly what the finished product being made will look like. This can be particularly helpful when dealing with complex geometries that difficult to interpret from a 2D drawing alone. Therefore, a mechanism that distributes the 3D data, designed in design division, to the world is required. Because broadband is still not popular in some regions in the world, 3D data compression and retrieval method is an important issue for reducing the latency of 3D data transmission with Internet access.

A number of methods have been developed to compress 3D surface models; Wakita et al. [9] adopted surface interpolation method using Gregory patches [8]. However, the surface interpolation method cannot be applied to the concave shapes or shapes with holes. To overcome this problem, Muraki et al. proposed a surface compression method using a surface fitting method [2,3]. In his paper, the data compression technique of 3D model is mentioned. However, any retrieval method is not evaluated and compressed file transfer is not performed.

In this paper, the performance of the 3D surface compression and retrieval algorithm based on a curve mesh interpolation [8] and N-side filling [2, 3] is evaluated. To be more concrete, an application system that transfers 3D surface models has been firstly developed. After that, the performance is evaluated with different network environments: such as third generation of mobile telecommunications (3G) and Worldwide Interoperability for Microwave Access (WiMAX). As the result, we confirmed the effectiveness of our compression method with practical data.

2. RELATED WORKS

2.1. Methods Based on the Surface Interpolation Method

The surface interpolation method is a method that generates a surface inside an area bounded by edges. In general, a four-sided area is interpolated with one surface. An N-sided area except for four-sided is

Taylor & Francis

interpolated with two or more surface patches. The inner curves are generated based on Catmull-Clark subdivision [1] and the N-sided region is divided into N quadrilateral regions. Then, a surface is interpolated to each of the generated regions. For example, Fig. 1 shows the control points of an N-sided area that generated based on Catmull-Clark subdivision method. In Fig. 1(a), three-sided area divided into 3 quadrilateral regions. In Fig. 1(b), five-sided area divided into 5 quadrilateral regions and six-sided area divided into 6 quadrilateral regions in Fig. 1(c). Each of the quadrilateral regions is smoothly interpolated with a Gregory patch. Therefore, in the surface interpolation method, each patch can be connected with G^1-continuity. Piegl et al. introduced an interpolation method with the angle tolerance ϵ to generate smooth surfaces [5]. In his method, it is possible to control the continuity between patches with the control points for connecting them between patches that are computed by the cross-boundary derivative. Yang et al. enhanced the Piegl's method to apply it to rational curve meshes [10]. In other research, Garcia et al. proposed the surface interpolation method of an arbitrary N-sided region by dividing the region into a star-shaped N-sided patch and quadrilateral patches. The size of the star-shaped N-sided patch can be controlled using parameter f. If the value of f increases, the N-sided region will be larger; and if the value of f decreases, the region will be smaller [6].

2.2. Methods Based on the N-side Filling Method

Tokuyama et al. proposed an N-side filling method [6] that covers an N-sided region with a B-spline surface. His method is the one that calculates the control points of the B-spline surface by using only the boundary edges of the surface. Since his technique is a basis of our research, a concrete procedure is described below:

1. Suppose a surface is applied to a closed region whose boundary edges are drawn in blue in Fig. 2(a). First, as shown in Fig. 2(a), four reference planes are generated outside of the closed region.
2. As shown in Fig. 2(b), the cross boundary derivatives are extended to the outside of the closed region, and the intersection points with four reference planes are generated.
3. As shown by the purple lines of Fig. 2(c), the intersection point sets generated in Step 2 are approximated with B-spline curve, and the boundary curves that cover an N-sided region are generated.
4. As shown by the purple points of Fig. 2(d), the sample points are generated on the lines that generated in Step 2.
5. As shown in Fig. 2(e), the control points of the B-spline surface are derived from the boundary curves generated in Step 3 and the sample

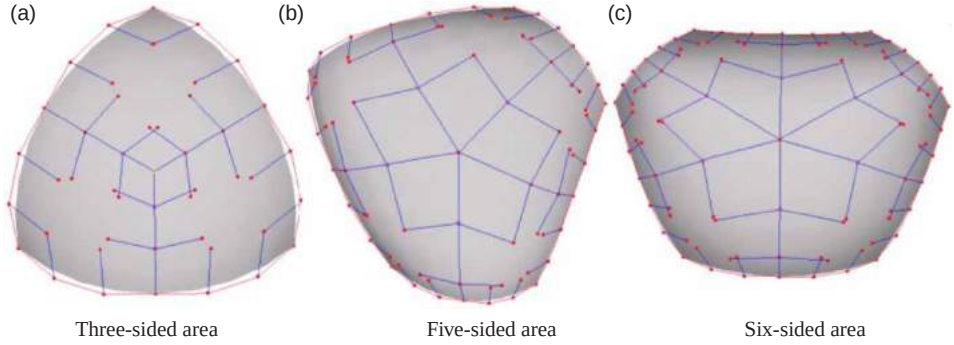

Fig. 1: Example of surface interpolation method application to the N-sided area.

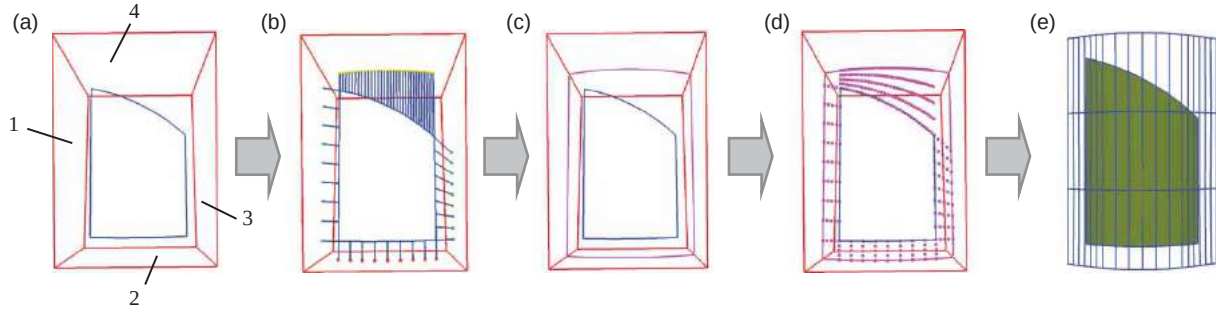

Fig. 2: The procedure of the N-side filling method.

points generated in Step 4 by using the least-squares method.

The Tokuyama's method, however, is not applicable to concave shapes. Therefore, Muraki et al. enhanced the N-side filling method for applying it to the shapes with holes or concave shapes and to maintain G^1-continuity with adjacent surfaces [2–4].

2.3. Surface Fitting Method with G^1-Continuity

Muraki et al. proposed a reconstruction method of trimmed surfaces for an N-side region with considering the G^1-continuity of adjacent surfaces [3]. His method unites the advantages of the surface interpolation method [8] and the N-side filling method [6]. In a common boundary where two surfaces are connected with G^1-continuity, the cross boundary derivatives are calculated based on the basis patch method [8] used in the surface interpolation method to generate the control points. The other control points in the surface are generated by approximating sample points by using the N-side filling method. The concept of this method is shown in Fig. 3. The blue markers show the control points calculated by the N-side filling method and the red markers show the ones calculated by the surface interpolation method. As shown in Fig. 3, by uniting the control points obtained by the two methods, it becomes possible to generate surfaces that are G^1-continuous with adjacent surfaces of concave shape or with holes. Moreover, by using the sample point generation method independent of the number of G^1-continuous boundary edges, it is possible to generate a surface surrounded by surfaces in all directions connecting with G^1-continuity.

The Muraki's method cannot apply directly to complex composite surface. One example is shown in Fig. 4. Fig. 4(a) shows a composite surface composed of 4×8 segments of Bezier surfaces. The composite surface is a twisted one. In Fig. 4(a), in some areas of the twisted surface, the normal vector is pointing to the opposite direction toward the average normal vector derived from the boundary curves. Due to this, the intersection points between the line segments and the reference planes cannot be calculated. In this study, we propose a method to divide such twisted composite surfaces to be fitted. Details are described in section 3.2.

3. DATA COMPRESSION AND RETRIEVAL

3.1. Concept of Our Proposed Method

The method proposed in this paper compresses 3D surface model data. Fig. 5 illustrates the main concept of our data compression and retrieval method.

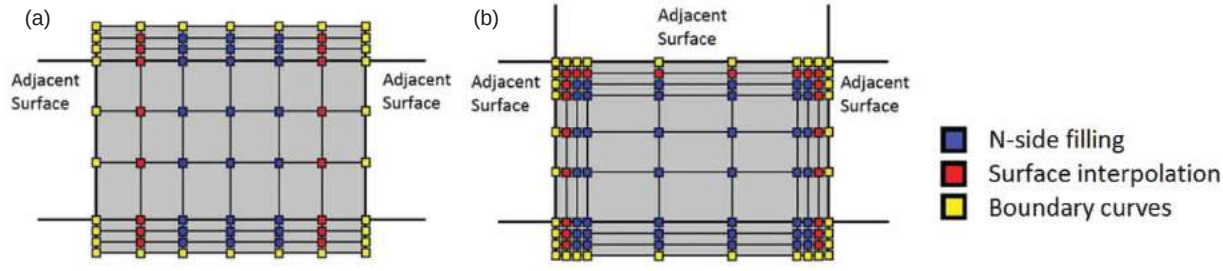

Fig. 3: Muraki's concept of surface fitting for a closed region: (a) Surface fitting to a closed region that has adjacent G^1-continuous surfaces in the left and right sides, (b) Surface fitting to a closed region that has adjacent G^1-continuous surfaces in the left, right and upper sides.

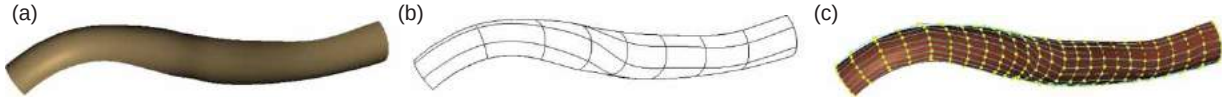

Fig. 4: (a) Example of a composite surface that cannot apply to the Muraki's method, (b) Segment lines of (a), (c) Control points of (a).

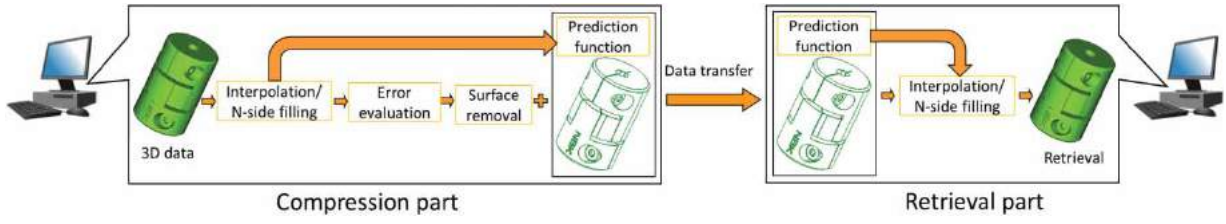

Fig. 5: Concept of 3D data compression and retrieval method.

In our method, the 3D data is compressed by estimating a surface that approximates from a boundary curve mesh, and then the original surface is deleted if the approximated surface is suitable. The compressed data can be retrieved from the boundary curve mesh in the same manner as the approximation of the compression process. To compress data easily, 3D surface type is classified into four elements; 1) Plane, 2) Interpolated surface, 3) Surface fitted with the N-side filling method, and 4) other surface. Elements 1) to 3) are generated from the boundary edges by using our approach. Element 4) represents the complex trimmed surface that is difficult to apply to the method described in section 2.3. The surface element is removed when the surface can be approximated within the tolerance. As the base surface of trimmed surface, contained in shape models, can be removed with this technique, it is possible to express the shape models with curve mesh representation. As a result, the amount of data is greatly reduced. The information of the method, the surface interpolation method or N-side filling method that should be applied to the four surface types, is indicated with the prediction function. The prediction function for the removed surface is added to the face as attribute information. The 3D shape model can be retrieved from the boundary curves with the prediction function.

Both our interpolation method and N-side filling method are difficult to apply to composite surfaces. It is difficult to fit a composite surface even in the case of the simple shapes whose boundary curves are closed to quadrilateral region. This is because the base surface has a large rough area or twisted boundary curves. Therefore, a composite surface must be appropriately divided after surfaces are generated and evaluated with the tolerance. If this operation is acceptable, the original surface elements are removed. Details of our data compression and retrieval algorithm are described in section 3.2. In our method, the surface element removal must be performed in the last stage of processing because the continuity of surfaces may collapse if it is performed in order. The compression stage of our method costs the calculation because the iterative calculations are required. For reducing the computational cost in the retrieval stage, some precalculated information is stored in the prediction function.

3.2. Compression and Retrieval

3.2.1. Flow chart of our compression part

Fig. 6 shows the flow of our compression process. The flow of the process is described as below:

1. Import all the surfaces to be compressed.
2. Judge for surface type 1) plane. By applying surface interpolation method or N-side filling method to the surface types 2) and 3), evaluate whether each surface is compressible or not. 3-sided region is judged whether can be interpolated with degenerated four-sided region and added to the surface type 2).
3. Save the value of the prediction function as the face attribute. The value of 1), 2) and 3) are set up as prediction function. Moreover, save some precalculated information along with the prediction function for reducing the computational cost in the retrieval stage. Details of this process is described in section 3.2.3.

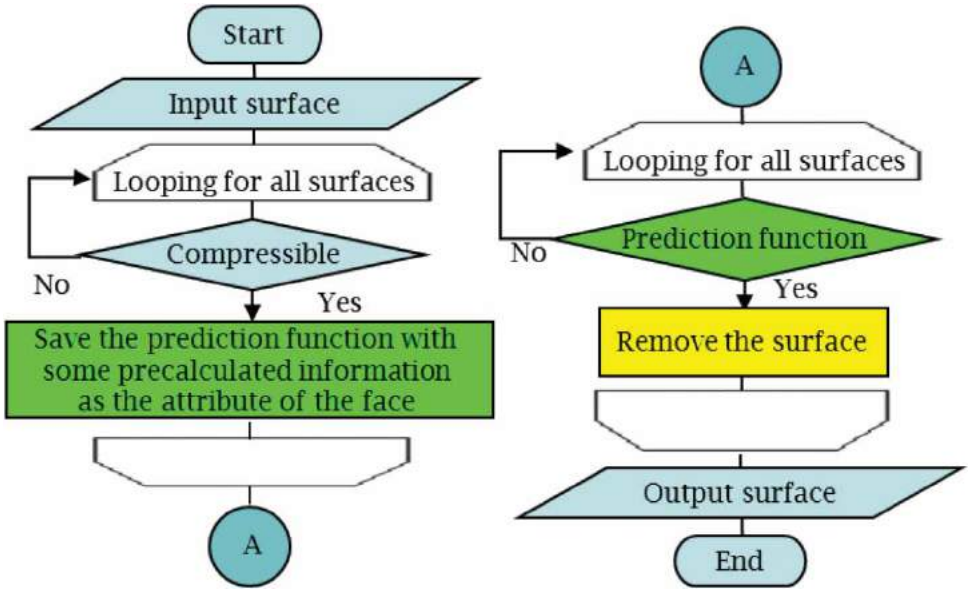

Fig. 6: Flow chart of our compression process.

4. Steps 2 and 3 are performed to all the surfaces.
5. According to the face attributes of 1) to 3), remove the surface data, and this step is performed to all the surfaces.
6. Output all the surfaces imported in step 1.

3.2.2. *Composite surface division*

As explained in section 3.1, it is difficult to fit a composite surface by using the method [2,3,4]. Accordingly, in our method, $n \times m$ segments that represent a composite surface is appropriately divided as preprocess. Our method is restricted to divide the non-trimmed composite surface only, because among the data used in our experiment, non-trimmed composite surfaces with huge data size are greatly affected on the compression ratio. Therefore, in our method, we divide a composite surface properly. However, the data amount will increase if the surface is divided, thus the division numbers for dividing the composite surface in n or m directions is determined by Eqn. (1), where *div_n* indicates the division number for direction n and *div_m* indicates that for direction m. The numbers of divisions are expressed in Eqn. (1) as follows:

$$\begin{aligned} div\_m = 2, div\_n = 2 \times n/m \quad & \text{if } n > m \\ div\_n = 2, div\_m = 2 \times m/n \quad & \text{if } n <= m \end{aligned} \tag{1}$$

By using Eqn. (1), the surface is divided and the surface fitting method is applied. The actual surface is divided only when the surface fitting is succeeded. Fig. 7 is the concept of composite surface division. Fig. 7(a) shows the composite surface with segments of 8×4 before division and Fig. 7(b) shows the composite surface with segments of 2×2 after dividing. The red line in Fig. 7(b) indicates the dividing line in the m direction; the green line shows the dividing line in the n direction. In addition, if surface fitting is successful, composite surface division will not be performed.

As shown in Fig. 8(a), in order to make composite surface with segments of 2×2 patches, the model shown in Fig. 4 is divided into 8 surfaces. Fig. 8(b) shows the boundary curves of the divided surface, and Fig. 8(c) is the result of surface fitting method application to each of the divided surfaces. We can see the surface is fitted with good accuracy. Fig. 8(d) shows the control points of the generated surfaces. We can find that the control points are not disturbed.

3.2.3. *Data retrieval part*

In data retrieval stage, the 3D surface model is retrieved from the boundary curves and the prediction function that is stored in the compression stage. In the compression stage, the error evaluation process is performed iteratively to make sure of the sufficiency of the generated surfaces. It is time consuming when the composite surface with the large number of control points is approximated, and the computational cost will be expensive. For avoiding these costs in the retrieval stage, it is necessary to add some practical information to the prediction function as attributes for generating surfaces. If the data size is reduced, the transmission time will be fast, but the retrieval cost will be high. For enhancing the time for retrieval, the precalculated information is used. To be more concrete, if the number of control points on approximated surfaces is more than a magical number N in the surface approximation process, the information that retrievals the surface are

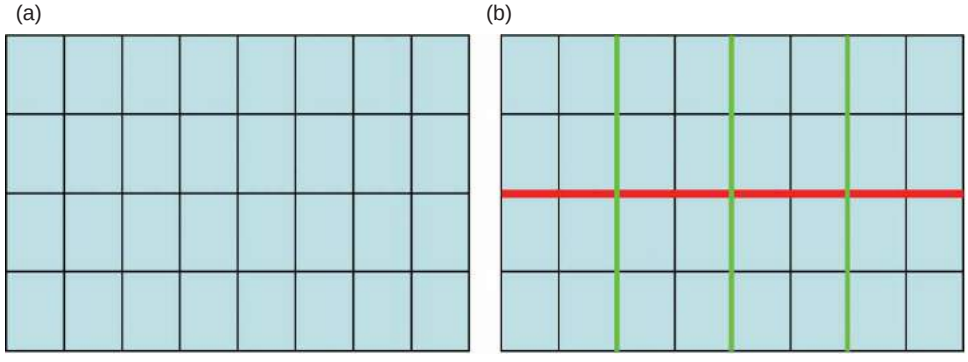

Fig. 7: Composite surface before and after division.

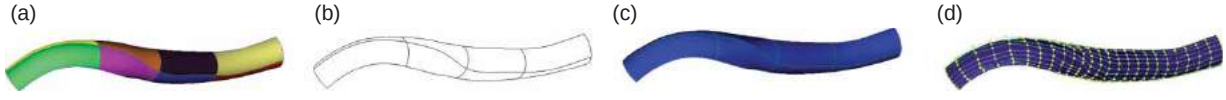

Fig. 8: (a) Result of the divided composite surfaces of Fig. 4, (b) Segment lines of the divided surface, (c) Result of the method [3] application to the each surface, and (d) Control points of the generated surfaces.

saved as the attributes. Processing for surface control point calculation by the N-side filling method is heavy. By adding such information to the attributes, the amount of computation can be reduced significantly. As the result, calculation cost of the surface generation can be reduced in the retrieval stage. Since the data size and calculation cost for retrieving surfaces are antinomy in each other, it is necessary to consider the balance of the data size and retrieval time by determining the added attributes with the number of surface control points. In our evaluation, in consideration of the balance between data size and retrieval time, the magical number N, which is stored as the attributes, is set to 20.

For example, Fig. 9 shows the retrieval of compressed data by using our surface fitting method. Fig. 9(a) represents the original IGES data. In Fig. 9(b), surfaces whose compression and retrieval are succeeded are shown in cyan and those for which compression is failed are shown in green. Fig. 9(c) shows only succeeded surfaces of Fig. 9(b).

Figs. 10(a) to (e) are the enlarged views of some data in Fig. 9. Fig. 10(a) shows the control points of the fitted surfaces by using the N-side filling method described in section 2.2. Fig. 10(b) shows interpolation for a 3-side region by using the method described in section 3.2. Figs. 10(c) to (e) show the fitted surfaces by using the surface fitting method described in section 2.3.

4. EXPERIMENTAL RESULT

Our method is applied to CAD data in the IGES format, and practicality is verified. Three of the experiment data are shown in Fig. 11. Fig. 12 shows the result of the data retrieval by using the method described in section 3.2.3. In Fig. 12, the surfaces for which data compression and retrieval are succeeded are shown in cyan. The surfaces for which compression is failed are shown in green. We can find that the surfaces are generated in good accuracy.

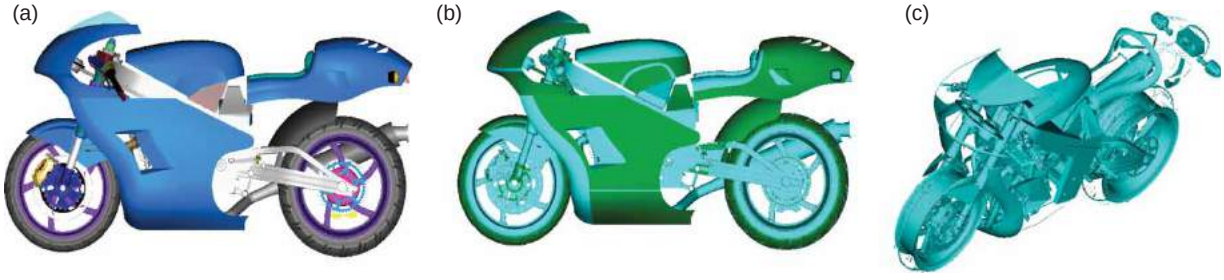

Fig. 9: Example of our surface fitting method application.

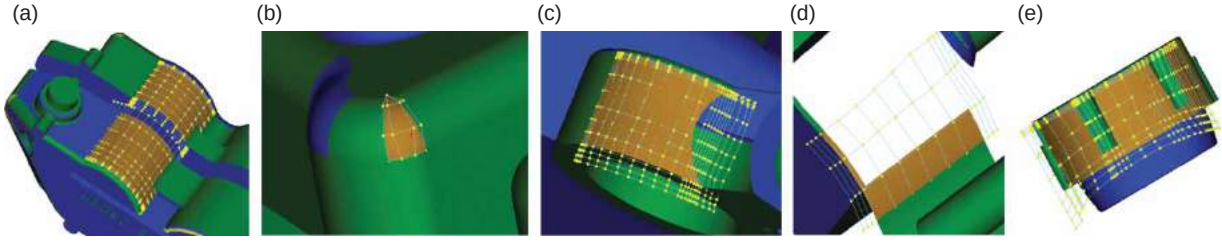

Fig. 10: Details of surface fitting.

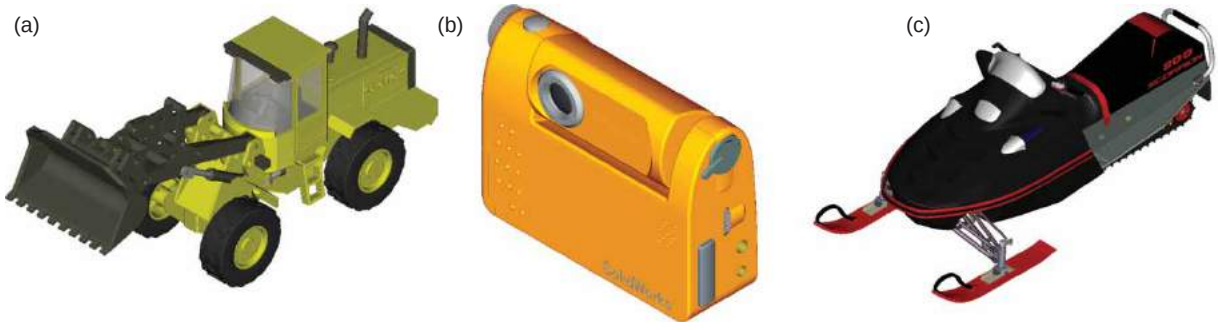

Fig. 11: CAD data used in the experiment: practical IGES data.

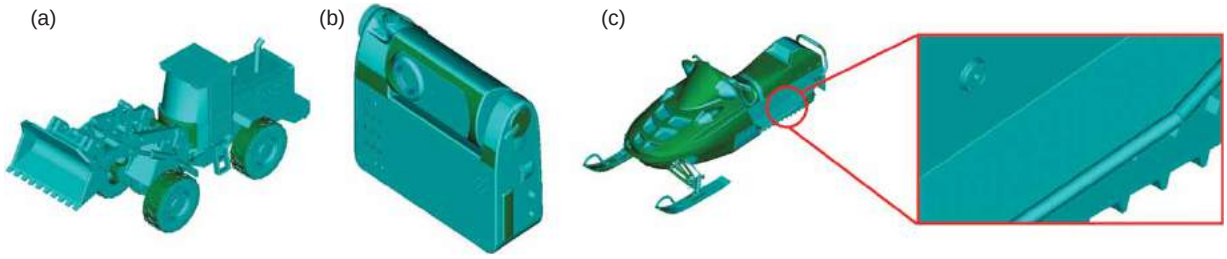

Fig. 12: Result of surface data retrieval: Our method is applied to the CAD data shown in Fig. 11 and the surface data is deleted and compressed. After that, the surface data is retrieved by using the boundary edges and the prediction function.

4.1. Performance Evaluation Method

The evaluation is carried out in three phases. Fig. 13 shows the flow of the evaluation. First, for each of the same shape, prepare IGES data and the compression data based on this technique. Next, compare the file size of IGES data compressed in the Zip format and the data compressed using our compression method. Then, upload those data on the web server and measure the download time and the retrieval time of the downloaded data. Two kinds of wireless devices, 3G and WiMAX, are used to measure the download time. Transmission speed of 3G is about 300Kbps in general and WiMAX is about 40 Mbps. We define the time required for three processes, import (decompression) of the downloaded data, retrieval, and display of the data on a CAD viewer screen as "retrieval time".

4.2. Evaluation Result by Data Size

In Fig. 14, data from A to H represent the practical CAD data used in our experiment. The size of three kinds of data, IGES data compressed in the Zip format, XVL data and our compressed data to which our method is applied are compared for performance evaluation. As shown in Fig. 14(a), blue bars represent IGES data and orange ones represent our data. In Fig. 14(b), purple bars represent XVL data and orange ones represent our data. We can find that the data size is significantly reduced by using our proposed compression method. For instance, in data F, the size of our data is approximately 26.7 times smaller than that of the IGES data. And also in dada F, the size of our data is approximately 1.4 times smaller than that of the XVL data.

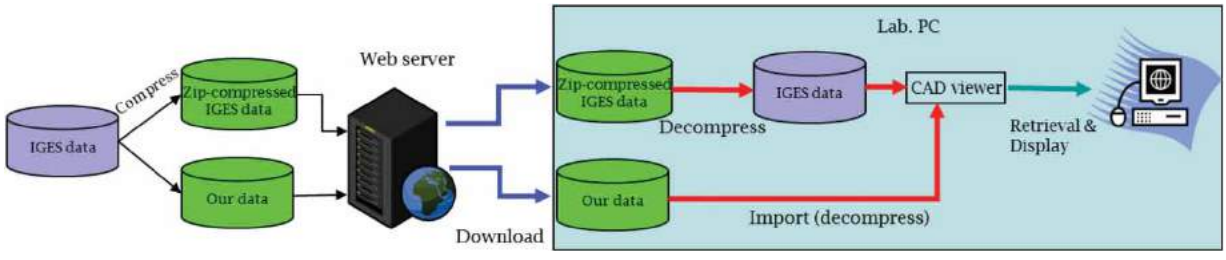

Fig. 13: Evaluation flow for the total time required to display practical data on the screen.

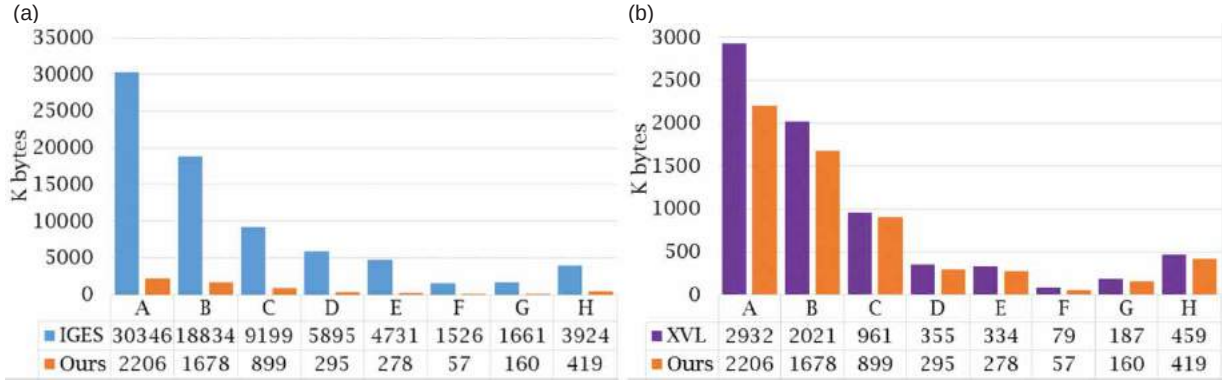

Fig. 14: Comparison of data size.

Tolerance (%)	A	B	C	D
10	1,819	1,648	768	292
1	2,206	1,678	899	295
0.1	2,597	1,792	915	306

Tab. 1: Comparison of data size (KB) with different tolerance values (%).

Moreover, we evaluated performance of our data compression method with the different set of tolerance values. In Tab. 1, the experimental data from A to D, is compared with different tolerance values (we employed 10, 1, and 0.1 (%)). In this paper, when ratio of the bounding box size and the maximum distance between source surface and generated surface is smaller than 1%, it is assumed that the surface is approximated in good accuracy [2]. Since our method is based on fitting a shape with information on tangent planes and boundary edges of the surface [2], it is apparent that significant surface can be generated even by increasing the tolerance. In addition, since the change of tolerance does not contribute significantly to compression, it is necessary to increase the pattern to be successful in the surface fitting. If

IGES data	Retrieval time (sec.)	Download time (sec.) (3G)	Display time (sec.)	Download time (sec.) (WiMAX 1.0 Mbps)	Display time (sec.)	Download time (sec.) (WiMAX 1.5 Mbps)	Display time (sec.)
A	54.81	1,350	1404.81	700	754.81	602	656.81
B	45.78	890	935.78	484	529.78	359	404.78
C	11.92	650	661.92	163	174.92	150	161.92
D	17.84	324	341.84	128	145.84	112	129.84
E	7.13	230	237.13	83	90.13	50	57.13
F	5.24	164	169.24	30	35.24	23	28.24
G	2.45	159	161.45	33	35.45	27	29.45
H	4.59	121	125.59	80	84.59	77	81.59

Tab. 2: Total display time for IGES data.

Our data	Retrieval time (sec.)	Download time (sec.) (3G)	Display time (sec.)	Download time (sec.) (WiMAX 1.0 Mbps)	Display time (sec.)	Download time (sec.) (WiMAX 1.5 Mbps)	Display time (sec.)
A	427.22	111	538.22	53	480.22	36	463.22
B	285.7	57	342.7	38	323.7	13	299.48
C	109.86	44	153.86	19	128.86	15	125.08
D	40.84	32	72.84	5	45.84	4	44.98
E	16.81	11	27.81	3	19.81	1	17.95
F	2.39	2	4.39	1	3.39	1	3.39
G	17.97	5	22.97	1	18.97	1	19.03
H	63.94	38	101.94	6	69.94	3	67.07

Tab. 3: Total display time for our data.

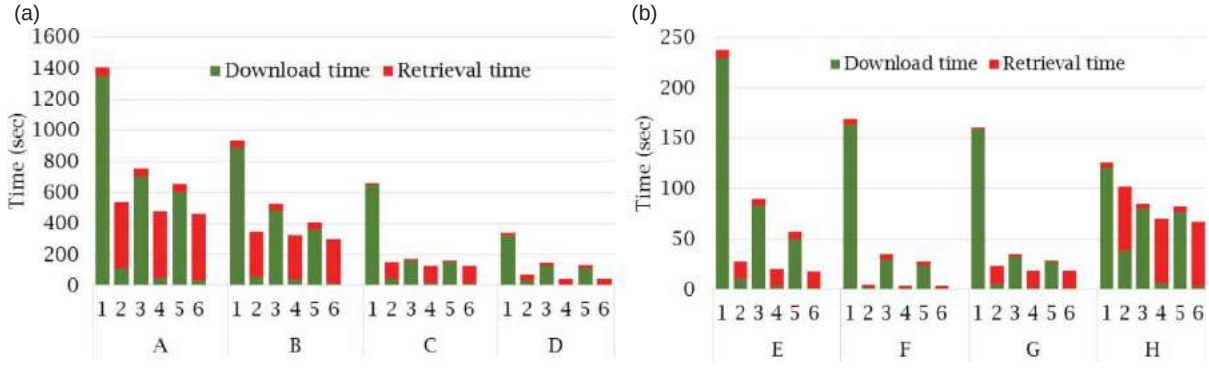

Fig. 15: (a) and (b) show comparison of data transmission time for IGES data and ours, odd numbers represent IGES data and even ones represent our data. Pairs of 1 & 2, 3 & 4, and 5 & 6 are the results of transmission time for 3G, WiMAX 1.0 Mbps and WiMAX 1.5 Mbps respectively.

the pattern increases, the compression ratio will be increase. Increase of the pattern is a topic for our future research.

4.3. Evaluation Result by Data Transmission Time

By using the method described in section 4.1, we evaluated our transmission system by measuring the download time and retrieval time of compressed IGES data and our data with 3G, WiMAX 1.0 Mbps and WiMAX 1.5 Mbps. The unit of time is second. As shown in Tabs. 2 and 3, the data transmission time of IGES data and our data is compared. Fig. 15 shows the graphs of Tab. 2 and Tab. 3. The green bars represent the download time and the red ones represent the retrieval time. Even though the retrieval time of our data is slower than the download time, overall performance of our data is faster than the IGES data. For example, in data F, the transmission time of our data is approximately 39 times faster than that of the IGES data in 3G environments, approximately 10 times faster with WiMAX 1.0 Mbps, and approximately 8 times faster than IGES data with WiMAX 1.5 Mbps.

5. CONCLUSION AND FUTURE WORKS

5.1. Conclusion

In this paper, we evaluated our compression and retrieval method by applying it to 3D surface models based on the curve mesh interpolation method and N-side filling method. Time of compression depends on data size only. The transmission time depends on data size and transmission speed. Since our method achieved high level compression, our method has advantages with big data and in low-speed network environment. We verified effectiveness of our method with practical data. As a result, despite of the different terminal speeds of network environment, our system can exchange gigantic data to a smaller size in a shorter time.

5.2. Future Works

As describe in section 3.2.3, the data size and calculation cost for surface retrieval are antinomy in each other, it is necessary to consider the balance of the data size and the retrieval time.

ACKNOWLEDGEMENTS

A part of the study is supported by the Adaptable and Seamless Technology transfer Program through targetdriven R&D (A-STEP).

REFERENCES

[1] Catmull, E.; Clark, J.: Recursively generated B-spline surfaces on arbitrary topological meshes, Computer Aided Design, 10(6), 1978, 350–355. http://dx.doi.org/10.1016/0010-4485(78)90110-0

[2] Muraki, Y.; Matsuyama, K.; Konno, K.; Tokuyama, Y.: Data Compression Method for Trimmed Surfaces Based on Surface Fitting with Maintaining G^1-Continuity with Adjacent Surfaces, Computer-Aided Design and Applications, 9(6), 2012, 811–824. http://dx.doi.org/10.3722/cadaps.2012.811-824

[3] Muraki, Y.; Matsuyama, K.; Konno, K.; Tokuyama, Y.: Reconstruction Method of Trimmed Surfaces with Maintaining G^1-continuity with Adjacent Surfaces, Computer-Aided Design and Applications, 11(2), 2014, 165–171. http://dx.doi.org/10.1080/16864360.2014.846085

[4] Muraki, Y.; Matsuyama, K.; Konno, K.; Tokuyama, Y.: A Study of Surface fitting Method of an N-sided Region Considering G^1-Continuity with Adjacent Surfaces, in Proceedings of IWAIT 2012

[5] Piegl, L.; Tiller, W.: Filling n-sided regions with NURBS patches, The Visual Computer, 15(2), 1999, 77–89. http://dx.doi.org/10.1007/s003710050163

[6] Pla-Garcia, N.; Vigo-Anglada, M.; Cotrina-Navau, J.: N-sided patches with B-spline boundaries, Computers & Graphics, 30(6), 2006, 959–970. http://dx.doi.org/10.1016/j.cag.2006.05.001

[7] Tokuyama, Y.; Konno, K.: Filling N-sided Region with a B-spline Surface, Information Processing Society of Japan, 43(10), 2002, 3209–3218.

[8] Toriya, H.; Chiyokura, H.: 3D CAD: Principles and Applications (Computer Science Workbench), Springer-Verlag, New York, Berlin, Tokyo, 1993. http://dx.doi.org/10.1007/978-3-642-45729-6

[9] Wakita, A.; Yajima, M.; Harada, T.; Toriya H.; Chiyokura H.: XVL: A Compact and Qualified 3D Representation With Lattice Mesh and Surface for the Internet, in Proceedings of the Web3D-VRML 2000 fifth symposium on 3D Web technology, Monterey, California, February, 2000, 21–24, ACM-Press. http://dx.doi.org/10.1145/330160.330174

[10] Yi-Jun, Y.; Jun-Hai, Y.; Hui, Z., Jean-Claude, P.; Jia-Guang, S.: A rational extension of Piegl's method for filling n-sided holes, Computer-Aided Design, 38(11), 2006, 1166–1178. http://dx.doi.org/10.1016/j.cad.2006.07.001